Spatial properties of koniocellular cells in the lateral geniculate nucleus of the marmoset *Callithrix jacchus*

Andrew J. R. White, Samuel G. Solomon and Paul R. Martin

Department of Physiology and Institute for Biomedical Research, University of Sydney, NSW 2006, Australia

(Received 18 October 2000; accepted after revision 25 January 2001)

1. The receptive field dimensions, contrast sensitivity and linearity of spatial summation of koniocellular (KC), parvocellular (PC) and magnocellular (MC) cells in the lateral geniculate nucleus (LGN) of 11 adult marmosets were measured using achromatic sinusoidal gratings.

2. The receptive field centre diameter of cells in each (PC, KC and MC) class increases with distance from the fovea. There is substantial overlap in centre size between the three cell classes at any eccentricity, but the PC cells have, on average, the smallest centres and the KC cells have the largest. Some PC and KC cells did not respond at all to the grating stimulus.

3. The contrast sensitivity of the receptive field centre mechanism in KC cells decreases in proportion to the centre area. A similar trend was seen for the surround mechanism. These characteristics are common to PC and MC cells, suggesting that they originate at an early stage of visual processing in the retina.

4. The KC cells showed, in general, lower peak evoked discharge rates than PC or MC cells. The spontaneous discharge rate of KC cells was lower than that of PC cells and similar to that of MC cells.

5. The majority of cells in all divisions of the LGN show linear spatial summation. A few cells did show non-linear spatial summation; these cells were predominantly located in the MC and ventral KC layers.

6. The ventral KC layers below and between the MC layers contain cells with larger and more transiently responding receptive fields than cells in the more dorsal KC layers.

7. We conclude that many of the contrast-dependent spatial properties of cells in the marmoset LGN are common to PC, MC and KC cells. The main difference between KC cells and the other two classes is that there is more variability in their response properties, and they are less responsive to high spatial frequencies.

The primate lateral geniculate nucleus (LGN) comprises parvocellular (PC) and magnocellular (MC) layers separated by small-celled koniocellular (KC) layers (Le Gros Clark, 1941; Bishop, 1984; Casagrande & Norton, 1991). The spatial receptive field properties of parvocellular (PC) and magnocellular (MC) pathway cells have been extensively described. The majority of MC and PC cells show centre–surround receptive field organisation. Compared to PC cells, the MC cells have relatively large receptive fields with high achromatic contrast sensitivity (for reviews see Kaplan *et al.* 1989; Lee 1996). The spatial properties of cells in the KC pathway have not been investigated systematically in any diurnal primate. In the nocturnal prosimian *Galago*, the receptive field properties of KC cells are more heterogeneous than those of PC and MC cells (Norton & Casagrande, 1982; Irvin *et al.* 1986, 1993; Norton *et al.* 1988; Xu *et al.* 2001). Some KC cells show centre–surround receptive field structure, but others do not, and the visual responses of some KC cells are modulated by tactile and auditory stimuli (Norton & Casagrande, 1982; Irvin *et al.* 1986, 1993; Norton *et al.* 1988). This led to the suggestion that the KC pathway is concerned with modulating visual input to the cortex rather than participating in conventional aspects of spatial vision (Casagrande, 1994). The goal of the present study is to compare quantitatively the spatial response properties of KC, PC and MC cells in a diurnal simian primate.

The common marmoset, *Callithrix jacchus*, is a New World monkey with a well-developed fovea and commensurately high (up to 30 cycles deg^{-1}) behavioural acuity (Walls, 1953; Ordy & Samorajski, 1968; Wilder *et al.* 1996). The midget (PC-projecting) and parasol (MC-projecting) ganglion cell populations in the marmoset are quantitatively comparable to those in Old World primates such as macaque (Goodchild *et al.* 1996). The response characteristics of PC and MC pathway cells in marmoset are similar to those of their counterparts in

macaque retina and LGN (Yeh *et al.* 1995; Kremers & Weiss, 1997; Kremers *et al.* 1997; White *et al.* 1998; Solomon *et al.* 1999). The marmoset LGN includes a well defined KC layer between the main PC and MC layers (Kaas *et al.* 1978; Spatz, 1978; Goodchild & Martin, 1998). This makes it possible to localise electrophysiological recordings to the KC division of the LGN in this species, and has enabled us to measure from a larger sample of KC cells than has been reported in previous studies. We previously described some of the chromatic and temporal response properties of KC cells in marmoset (White *et al.* 1998; Solomon *et al.* 1999). Here, we describe responses to sinusoidal spatial contrast modulation. The responses of most KC cells for this type of stimulus are shown to be substantially similar to those of PC and MC pathway cells. Some of these results have been published in abstract form (Martin *et al.* 1999).

METHODS

Animal preparation

Recordings were made from 11 adult marmosets (*Callithrix jacchus*; body weight 250–370g). Animals were obtained from the Australian National Health and Medical Research Council (NHMRC) combined breeding facilities in Adelaide and Melbourne. Three of the animals were male, the others female. All procedures used conform to the provisions of the Australian NHMRC code of practice for the care and use of animals. Animals were initially sedated with isoflurane (Forthane, Abbott, Sydney, 1.5–2%) then anaesthetised with intramuscular ketamine (Ketalar, Parke-Davis, Sydney, 30 mg kg^{-1}) for surgery. A femoral vein and the trachea were cannulated. Animals were artificially respired with 70 % NO_2–30 % carbogen (5 % CO_2 in O_2). A venous infusion of 40 mg kg^{-1} h^{-1} alcuronium chloride (Alloferin, Roche, Sydney) was given in dextrose Ringer solution to maintain neuromuscular block of the skeletal muscles. Anaesthesia was maintained during recording by intravenous infusion of sufentanil citrate (Sufenta-Forte, Janssen-Cilag, Beerse, Belgium, 4–8 mg kg^{-1} h^{-1}), with supplemental isoflurane (Forthane, Abbott, Sydney, 0.25–1%) as required. Electroencephalogram and electrocardiogram signals were monitored to ensure adequate depth of anaesthesia. End-tidal CO_2 was measured and maintained near 4 % by adjusting the rate and stroke volume of the inspired gas mixture. The pupils were dilated with topical neosynephrine (Sterling-Winthrop, New York). Penicillin (Aquacaine, CSL Australia, Melbourne, Australia) and corticosteroids (Decadron, Merck, Sharpe & Dohme, Sydney, Australia) were administered daily.

The animal was mounted in a stereotaxic headholder. The eyes were protected with oxygen-permeable contact lenses. Appropriate corrective lenses were used to focus the eyes on a tangent screen 114 cm away. Refraction was optimised by measuring the response to grating stimuli of the first parvocellular cell encountered and then selecting the corrective lens that maximised the cell's spatial resolution. A 2 mm artificial pupil was routinely used. The stereotaxic frame was tilted to bring the optic axis close to the horizontal plane. The positions of the fovea and optic disk were mapped onto the tangent screen with the aid of a fundus camera equipped with a rear projection device. The table supporting the stereotaxic frame could be rotated as required to bring the receptive fields of recorded cells close to the centre of the tangent screen. Such movements were monitored by means of a laser attached to the table.

A craniotomy was centred over coordinates AP 5.0 mm, Lateral 7.0 mm (Stephan *et al.* 1980) and a microelectrode (parylene-coated tungsten or glass-coated steel; impedance 5–12 MΩ, F. H. Haere Co, Bowdoinham, ME, USA) was lowered into the LGN. Action potentials arising from visually responsive units were identified (Bishop *et al.* 1962). The time of their occurrence was measured with an accuracy of 0.1 ms and stored.

Visual stimuli

Each visually responsive cell was initially characterised using hand-held stimuli and the receptive field position was marked on the tangent screen. A front-silvered mirror was then interposed between the eye and the receptive field position. This mirror reflected the image of a cathode ray tube (CRT) monitor placed to give an optical path length of 114 cm. Achromatic sine wave gratings with spatial frequency between 0.12 and 15.6 cycles deg^{-1} were presented on the CRT. In early experiments the stimuli were generated on an Apple Macintosh 7300/200 computer using the Brainard/Pelli pixel toolbox (Brainard, 1997) and Matlab (Mathworks Inc., Natick, MA, USA) software and presented on an Apple CM-1565 MCLR monitor (luminance 13–29 cd m^{-2}) at a frame refresh rate of 67 Hz. In later experiments stimuli were generated using a VSG series 3 video signal generator (Cambridge Instruments, Rochester, UK) and presented on a Barco CCID 121 monitor (mean luminance 60 cd m^{-2}) at a frame refresh rate of 100 Hz. No systematic differences in response properties were apparent when data collected from the different stimulators were compared. The results have been pooled for the present study. Note that the small size of the marmoset eye (Troilo *et al.* 1993) means that retinal flux will be higher than that of humans for a given stimulus intensity. The temporal frequency for drifting gratings was either 3.3 or 4 Hz. Stimuli were presented in a square or circular aperture that subtended 8–12 deg. Responses to stimuli presented in smaller apertures were also tested for a few cells.

A spatial frequency tuning curve for each cell was measured using high contrast (60–98 % Michelson contrast) gratings. The contrast–response function at the optimal spatial frequency was then measured. For cells that showed significant response saturation, a spatial frequency tuning curve was measured at a contrast in the linear part of the contrast–response range. Linearity of spatial summation was tested with counterphase modulated gratings. The temporal modulation frequency for counterphase gratings was 3.68 Hz. The spatial frequency used for the linearity test was at or above the optimal spatial frequency for the cell. Orientation and direction tuning were measured using drifting gratings at the optimal spatial frequency presented at 16 different orientations in a pseudo-random order. A spatial frequency tuning curve was then measured at a range of interleaved contrasts in order to obtain a spatial contrast modulation transfer function.

Temporal contrast sensitivity was measured for the majority of cells as described fully elsewhere (Solomon *et al.* 1999). The stimulus was a large (6.4 deg) spatially uniform field consisting of the combined image of red and green light-emitting diodes (LEDs) presented in Maxwellian view. The LEDs were modulated in phase at temporal frequencies between 0.98 and 64 Hz. Contrast was varied with a sine envelope over 8.192 s (for 0.98 Hz modulation frequency) or 4.096 s (for other modulation frequencies). The time averaged luminance was close to 1000 photopic Trolands.

Response analysis

A peristimulus time histogram (PSTH) was constructed from 5–10 s of evoked response for each stimulus condition. A fast Fourier transform (FFT) was taken from each PSTH and the first harmonic amplitude was used to estimate cell responsivity. Function fitting was carried out using least-squares error minimisation (Simplex algorithm, Matlab optimisation toolbox; MathWorks Inc.). Where appropriate, starting parameters close to the expected solution for the numerical search were set by an operator before optimisation. This procedure avoided convergence to local minima in the multivariate data space.

Histological processing

The position of each recorded cell was noted by reading the depth from the hydraulic microelectrode advance (David Kopf Model 640, Tujunga, CA, USA). Electrolytic lesions (6–20 μA, 6-20 s, electrode negative) were made to mark selected locations on electrode tracks. At the conclusion of recording, the animal was killed with an overdose of pentobarbitone sodium (80–150 mg kg^{-1}, I.V.) and perfused intracardially with 0.25 l of saline (0.9% NaCl). This was followed by 0.3 l of freshly prepared 4% paraformaldehyde in 0.1 M phosphate buffer (PB, pH 7.4) The brain was removed and placed in 4% paraformaldehyde in PB for 12 h, then placed in 30% sucrose in PB until it sank. Coronal sections of 30 μm thickness were cut on a freezing microtome. Alternate sections were mounted onto glass slides, air dried, then stained for Nissl substance. The position of recorded cells was reconstructed by identifying the electrolytic lesions and correlating changes in eye dominance with the laminar pattern revealed by the Nissl stain (White *et al.* 1998). The position of each recorded cell with respect to the laminar borders was also calculated (White *et al.* 1998).

Nomenclature

We use the nomenclature of Kaas *et al.* (1978) to distinguish two anatomical subdivisions of the KC pathway. These are subdivision Ipm, which lies between the PC and MC layers, and subdivision S, which lies ventral to the MC layers. An alternate naming scheme (Ding & Casagrande, 1997; Hendry & Reid, 2000) identifies each part of the KC division according to its ventro-dorsal rank in the LGN layers, so S is equivalent to K1, and Ipm is equivalent to K3.

RESULTS

Data were obtained from 146 cells. We classified visually responsive units as belonging to PC, KC or MC divisions of the LGN if the reconstructed recording site could be clearly localised with respect to the laminar borders, and did not lie within 10% depth of a laminar border. This criterion reduces the sample size but at least partially compensates for positional uncertainties which accompany the anatomical reconstruction (White *et al.* 1998). A total of 91 units (44 PC; 12 MC; 35 KC) met this criterion. We maximised our yield of KC cells by using relatively high impedance electrodes (10–15 MΩ) and by selecting regions in the posterolateral LGN where the KC layers are vertically oriented (Kaas *et al.* 1978; White *et al.* 1998).

A Nissl stained coronal section through the marmoset LGN approximately midway along the antero-posterior axis is shown in Fig. 1*A*. The KC subdivision is visible as a relatively cell-sparse zone between the PC and MC layers. The path of the recording electrode is superimposed on the section to show the position of visually responsive units encountered in a single penetration.

Spatial frequency response tuning curves for a PC, KC and MC cell encountered in this electrode penetration are shown in Fig. 1*B–D*. Stimulus contrast was 100%. The PC and MC cell

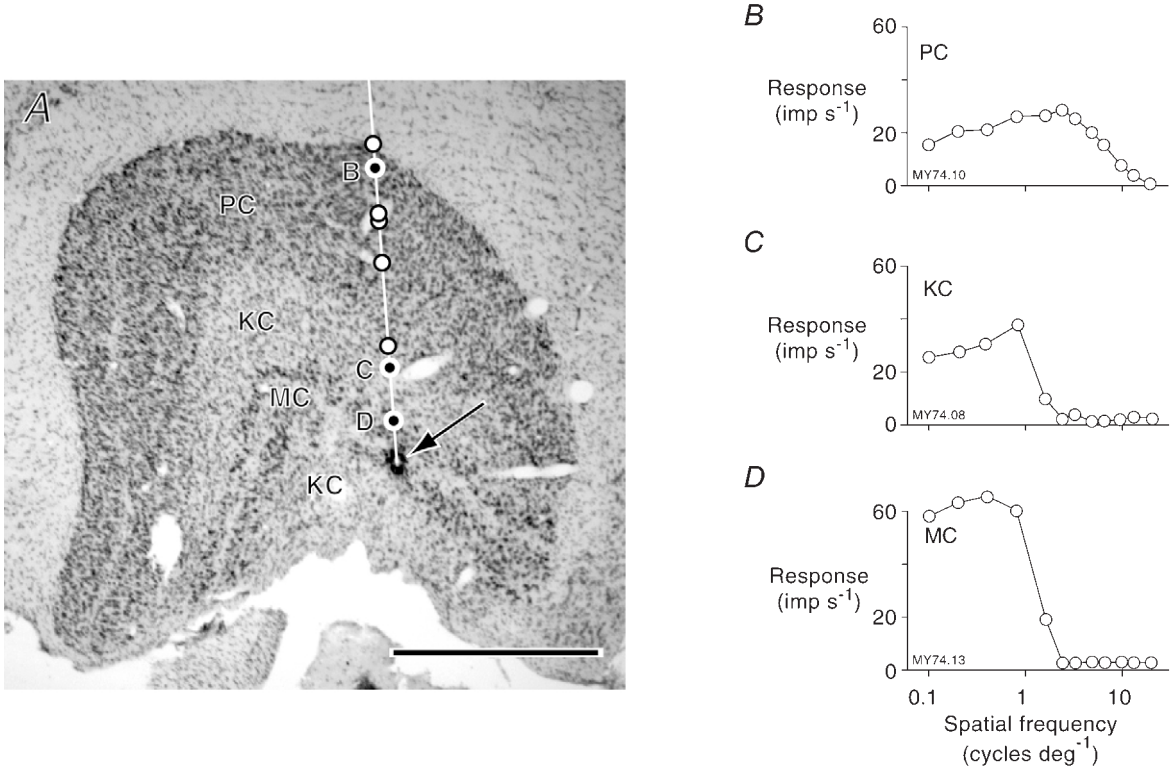

Figure 1. Localisation of responses

A, coronal section of the right LGN of a female marmoset. The path of an electrode penetration is shown by the white line. Open circles show the location of visually responsive units. The end of the penetration (in the external MC layer) is marked by an electrolytic lesion (arrow). Scale bar 1 mm. Spatial frequency response tuning curves of three of the visually responsive units encountered in this penetration are shown in *B–D*. The PC cell (*B*) responds to higher spatial frequencies than the KC cell (*C*) or the MC cell (*D*). The KC cell responds at relatively low amplitude throughout its activation range.

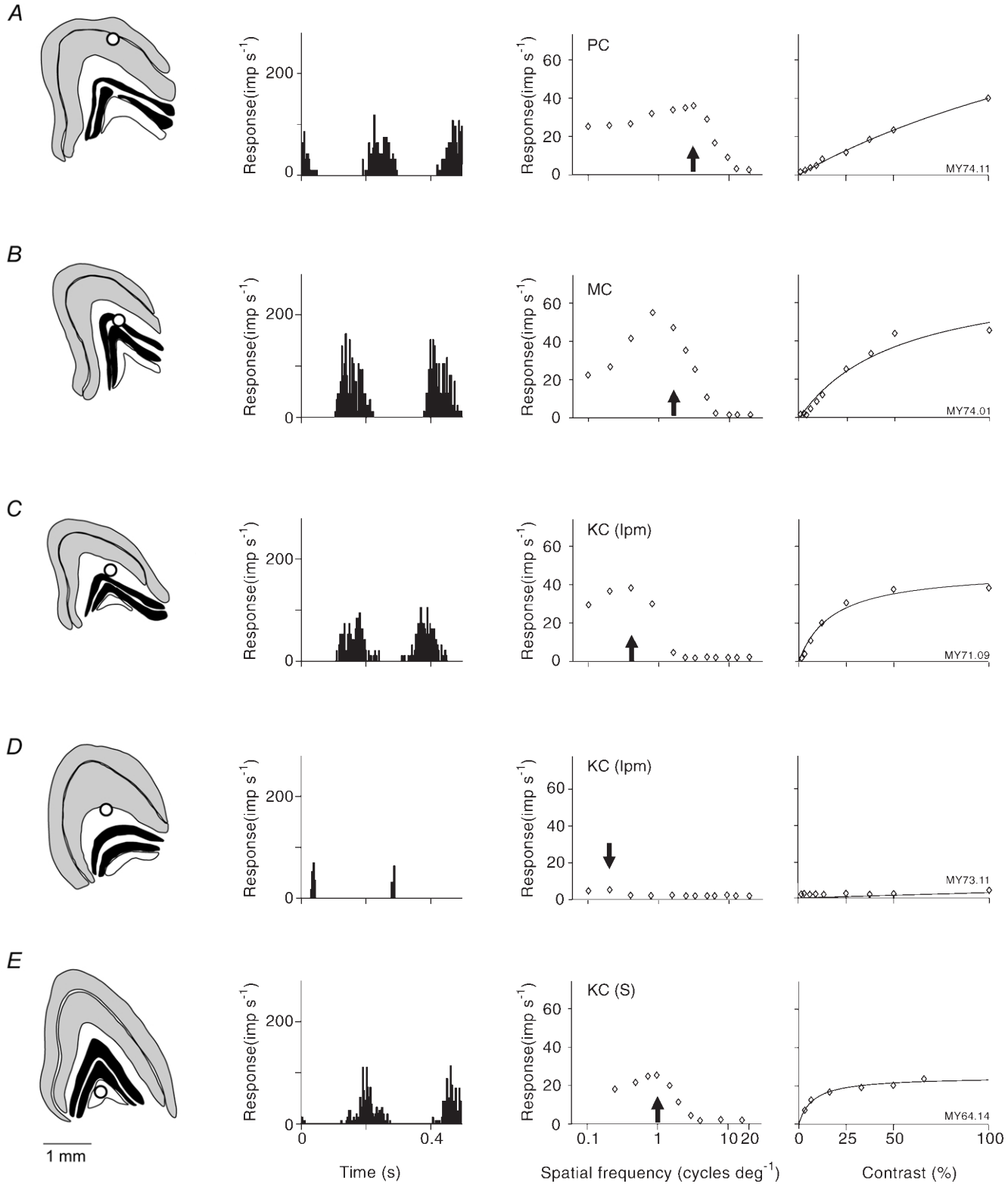

Figure 2. Heterogeneity of visually evoked responses in the KC layers

The recording site within the LGN is shown for each of five cells (left panel). ▨, PC; □, KC; ■, MC. The peristimulus time histograms show two cycles of the cell's response to a high contrast grating of optimal spatial frequency. The spatial frequency tuning curve for each cell is shown in the centre panels. A contrast–response function at optimal spatial for each cell is shown in the right panel. The spatial frequency used was close to optimal (arrow on spatial tuning curve). The line shows the best fitting solution of the Naka-Rushton function, as described in the text. The three KC cells (*C–D*) exhibit a variety of response behaviours; in comparison with a typical PC cell (*A*) and MC cell (*B*) they show low

responses conform nicely to expectation: the PC cell responds to higher spatial frequencies than the MC cell but the MC cell responds more vigorously to low spatial frequencies (Derrington & Lennie, 1984; Kremers & Weiss, 1997; Usrey & Reid, 2000). The spatial bandwidth of the KC cell resembles that of the MC cell but the response amplitude is lower throughout the tested range. These examples typify the pattern of responses seen in the three divisions of the LGN.

Spatial frequency tuning

Figure 2 illustrates the range of response properties seen in KC cells. Example PSTH and spatial tuning curves for three KC cells are shown (Fig. 2*C–E*) together with contrast–response functions measured at the optimal spatial frequency. Typical responses of PC (Fig. 2*A*) and MC (Fig. 2*B*) cells are shown for comparison. In comparison to the relatively stereotyped response properties of PC and MC cells, a range of behaviour was measured for KC cells: some KC cells respond vigorously to low and intermediate spatial frequencies (Fig. 2*C*) whereas the response of other KC cells to any spatial contrast is feeble (Fig. 2*D*). As previously shown for PC and MC cells (Derrington & Lennie, 1984; Croner & Kaplan, 1995; Yeh *et al.* 1995; Kremers & Weiss, 1997), the contrast–response function of KC cells to spatial contrast can be well accounted for by a saturating hyperbolic ('Naka-Rushton') function of the form:

$$R(C) = R_{\mathrm{m}}C/(b + C), \quad (1)$$

where C is contrast, R_{m} is the maximum response amplitude and b is the contrast eliciting half the maximal response (Naka & Rushton, 1966). As in our previous study of responsivity to temporal modulation (Solomon *et al.* 1999), we found this function to give the best account of contrast–response relationships with the minimum number of free parameters. The goodness of fit was assessed by comparing the magnitude of residual errors (MSE) normalised to peak firing rate. No significant difference was seen (ANOVA single factor $P = 0.14$) when the cell classes were compared (PC: 0.89, S.D. 1.05, $n = 27$; KC: 2.50, S.D. 5.24, $n = 11$; MC: 3.65, S.D. 4.68, $n = 6$). We fixed the response to pass through zero at zero contrast. Adding a third free parameter to translate the contrast–response function on either the x-axis ('contrast threshold') or y-axis ('spontaneous activity') produced insignificant improvement in the residual error values for each curve (data not shown). The predicted maximal response of KC cells was lower than that of PC or MC cells (R_{m}: PC: 88.9, S.D. 183.9, $n = 27$; KC: 40.4, S.D. 23.5, $n = 11$; MC: 53.7, S.D. 21.4, $n = 6$). As for MC cells, the majority of KC cells showed response saturation for high (> 50%) contrast stimuli (b: PC: 207.5, S.D. 451.9; $n = 27$; KC: 33.9, S.D. 65.5, $n = 11$; MC: 38.7, S.D. 18.6, $n = 6$). There is, however, substantial overlap in these parameters for the three cell groups and there is no statistical significance (ANOVA single factor $P > 0.1$).

Spatial resolution

Spatial resolving capacity was estimated by fitting a spline function to the upper limb of the spatial frequency–response curve for each cell, and finding the frequency at which that function fell below 5 impulses (imp) s^{-1}. The result is shown in Fig. 3*A*. Our estimate of spatial resolution in PC and MC pathway cells is consistent with other estimates in marmoset (Kremers & Weiss, 1997), with PC cells generally showing higher resolution than MC cells. The KC cells have, on average, the lowest cut-off frequency at any eccentricity, but there is substantial overlap with both PC and MC groups. The cut-off frequency for PC cells and KC cells decreases significantly with eccentricity (PC resolution = $6.81 \times \mathrm{eccentricity}^{-0.312}$, $r^2 = 0.17$, $P < 0.02$; KC resolution = $5.32 \times \mathrm{eccentricity}^{-0.428}$, $r^2 = 0.51$, $P < 0.02$); the decrease is also significant for MC cells (MC resolution = $3.25 \times \mathrm{eccentricity}^{-0.249}$, $r^2 = 0.58$, $P < 0.02$) but the sample ($n = 10$) is small. The same pattern of results was obtained when the criterion value was set to a fixed percentage (5%) of the peak firing rate for each cell (data not shown).

Peak and maintained discharge rate

Koniocellular pathway cells in *Galago* are characterised by relatively low peak firing rate and low rates of maintained discharge (Irvin *et al.* 1986). We asked whether this distinction also holds for KC cells in the marmoset. We measured peak firing rate in a 28 ms Gaussian-averaged window at the optimal spatial frequency for high contrast stimuli, and maintained discharge (measured from Fourier component F0) for a uniform field at the space-average luminance of the modulated gratings. Figure 2*B* and *C* shows the result. There are no significant differences between the cell groups in the mean values for either parameter (peak rate PC: 84.8, S.D. 34.1; KC: 81.7, S.D. 40.0; MC: 100.6, S.D. 53.0; maintained rate PC: 10.3, S.D. 6.0; KC: 8.8, S.D. 10.5; MC: 7.0, S.D. 6.8). As Fig. 2*B* and *C* shows, the different cell groups show distinct distributions of these parameters. Peak firing rate is skewed towards values below 60 imp s^{-1}) for KC cells in comparison with MC and PC cells ($P < 0.02$, χ^2 statistic) and maintained discharge rate for PC cells (10.0 imp s^{-1} exceeds the grouped mean value for MC and KC cells (9.3 imp s^{-1}; $P < 0.05$, χ^2 statistic).

Centre and surround dimensions

A spatial frequency tuning curve was measured at a contrast in the linear part of the cell's contrast–response function for a total of 54 units (PC, $n = 27$; KC, $n = 22$; MC, $n = 12$). Receptive field dimensions were estimated using a difference-of-Gaussians (DOG) function (Rodieck, 1965; Enroth-Cugell & Robson, 1966; Derrington & Lennie, 1984; Croner & Kaplan, 1995). Response amplitude to the (suprathreshold) stimulus was predicted in the spatial frequency domain as described by Croner & Kaplan (1995):

$$R = C((K_c\pi r_c^2 e^{-(\pi r_c f)^2}) - (K_s\pi r_s^2 e^{-(\pi r_s f)^2})), \quad (2)$$

maximum response amplitude (*D* and *E*) and response saturation at intermediate and high contrasts (*C* and *E*). Scale bar 1 mm; grating drift frequency 3.3 Hz. Fit parameters (R_{m}, b, gain): *A*: 139, 246.8, 0.56; *B*: 76, 52.8, 1.44; *C*: 39, 28.6, 1.38; *E*: 26, 7.5, 3.53. No satisfactory fit was found for the cell in *D*.

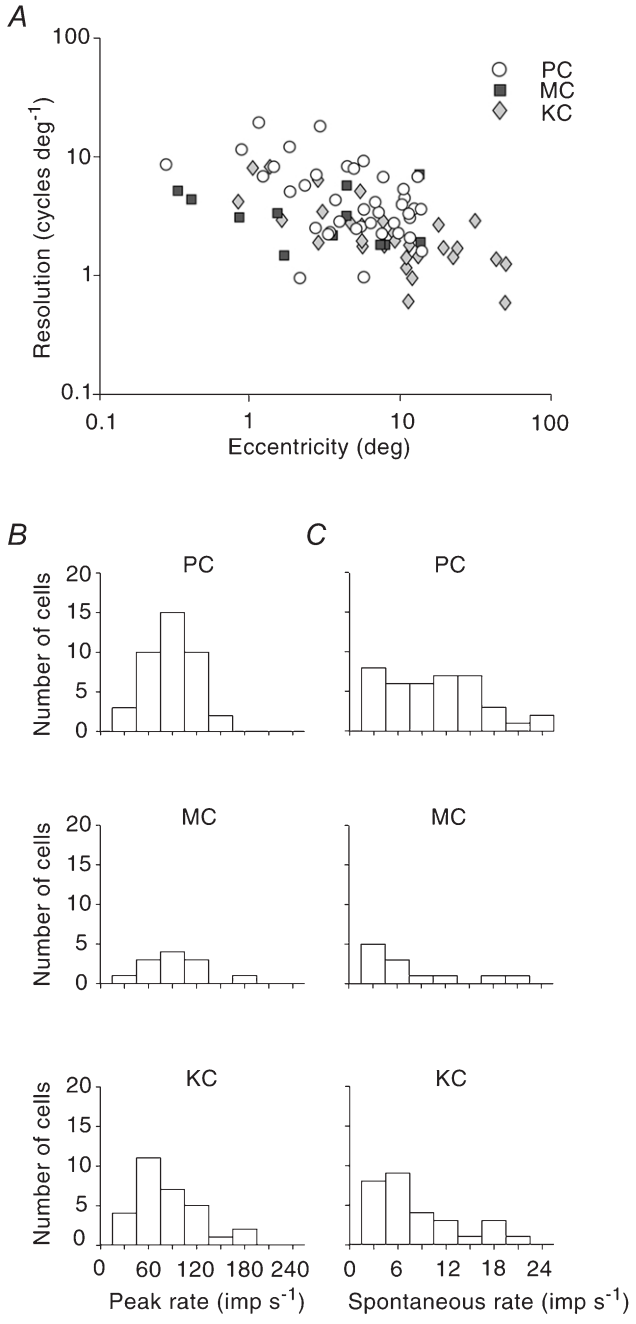

Figure 3. Comparison of response properties

Spatial resolution (cut-off spatial frequency) for high contrast gratings is shown in *A*. At a given eccentricity, PC cells have the highest spatial resolution, but there is substantial overlap between the PC, KC and MC populations. *B*, peak discharge rate for high contrast gratings at optimal spatial frequency. The proportion of KC cells showing low (< 60 imp s^{-1}) peak firing rate is greater than that of PC or MC cells. *C*, maintained discharge rate for uniform illumination. The proportion of PC cells showing high (> 10 imp s^{-1}) maintained discharge is greater than that of MC or KC cells.

where R is the response amplitude (imp s^{-1}), C is the Michelson contrast of the stimulus and f is the spatial frequency of the stimulus. The free parameters K_c, K_s, r_c and r_s were optimised using least-squares minimisation (see Methods). Parameters r_c and r_s are Gaussian centre and surround radius (where the sensitivity falls to 1/e of the maximum). Parameters K_c and K_s are centre and surround peak sensitivity, expressed as the contribution to the cell response (in imp s^{-1}) of a unit area of the centre and surround mechanism. Response amplitude was scaled by the stimulus contrast to give responsivity (imp s^{-1} (% contrast)$^{-1}$) as a function of spatial frequency for each cell.

Figure 4 shows examples of responses with the best-fitting DOG function for PC, KC and MC cells. The DOG model can account for the responses of MC and PC cells in marmoset LGN (Kremers & Weiss, 1997). We found that it also provides a good description for the majority of cells tested in the KC layers. Some cells (PC, $n = 3$; KC, $n = 2$) were clearly responsive to hand-held visual stimuli and yet did not reach the criterion response level of 10 imp s^{-1} for any grating stimulus. Furthermore, the responses of a proportion of cells in each group (PC, $n = 5$; KC, $n = 7$; MC, $n = 1$) were best accounted for when the sensitivity of the surround mechanism was set to zero (e.g. Fig. 4*D*). Responsivity in these cells may have been suppressed by the large stimulus field; evidence in favour of this suggestion is given below. As was the case for spatial resolution, the centre size of all cell groups increased with visual field:

PC: $r_c = 0.006 \times$ eccentricity $+ 0.075$, $r^2 = 0.145$, $P < 0.02$;
KC: $r_c = 0.007 \times$ eccentricity $+ 0.131$, $r^2 = 0.443$, $P < 0.02$;
MC: $r_c = 0.006 \times$ eccentricity $+ 0.092$, $r^2 = 0.165$, $P = 0.19$.

The size of MC and PC cell receptive field centres is close to that reported for marmoset by Kremers & Weiss (1997).

We also measured low frequency roll-off as described by Irvin *et al* (1993). Response amplitude at the optimal spatial frequency was compared with amplitude at a spatial frequency 0.5 log units below optimal. The average roll-off was 77.4 % of the peak response for PC cells (S.D. 16.3, $n = 29$), 74 % for MC cells (S.D. 22.2 %, $n = 7$) and 76.9 % for KC cells (S.D. 22.7 %, $n = 22$). A one-way ANOVA test showed no difference between the three groups ($P = 0.91$).

Receptive field size and contrast sensitivity

Further evidence that the spatial properties of KC pathway cells have fundamental similarities to those of PC and MC cells is given by the relationship of receptive field size and contrast sensitivity, as follows. If centre sensitivity is plotted against receptive field radius on a double logarithmic scale, a regression line with a slope of -2 is attained when the centre sensitivity is inversely proportional to centre area (Enroth-Cugell & Shapley, 1973; Cleland, 1983; Irvin *et al.* 1993; Croner & Kaplan, 1995; Levick, 1996). When this relationship holds, the integrated sensitivity ('volume') of the centre mechanism is independent of the receptive field radius. The radius–contrast sensitivity relationship for our cell sample is

shown in Fig. 5. The data for PC and MC cells are broadly in agreement with studies of PC and MC receptive fields in the marmoset (Kremers & Weiss, 1997) and macaque (Croner & Kaplan, 1995), and with all LGN cell groups in the prosimian *Galago* (Irvin *et al.* 1993). As Fig. 5 shows, the KC cell population in marmoset follows the same trend. The dashed lines show the ideal relationship with slope −2. The regression line (Fig. 5*A*, continuous line) for all cells is:

$$K_c = 0.617\, r_c^{-1.581}\ (r^2 = 0.48,\ P < 0.02),$$

where K_c is the peak contrast sensitivity for the receptive field centre and r_c is the receptive field centre radius in

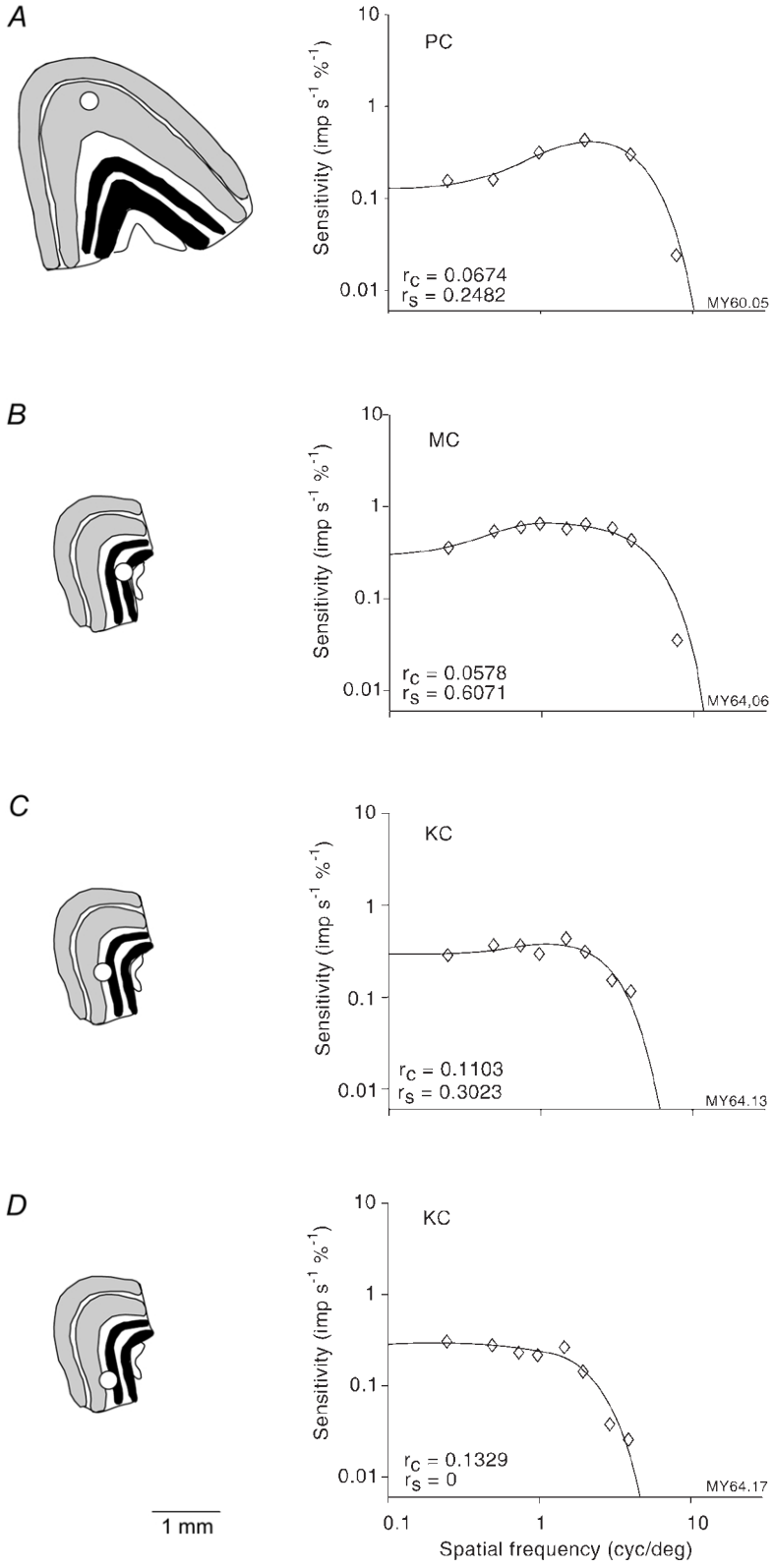

Figure 4. Contrast sensitivity of PC, MC and KC cells

The left panels show for each of four cells the recording site in the LGN. ▨, PC; □, KC; ■, MC. Stimulus contrast was within the linear response range for each cell. The right panels show responsivity. The continuous line shows the optimal solution to the difference-of-Gaussians (DOG) equation as described in the text (eqn (2)). The derived values for centre radius (r_c) and surround radius (r_s) are shown on each plot. *A*, PC cell, eccentricity 2.81 deg. *B*, MC cell, eccentricity 13.41 deg. *C*, KC cell, eccentricity 5.69 deg. *D*, KC cell, eccentricity 8.98 deg. Note that for this cell no evidence for a surround mechanism is given by the DOG model.

degrees). The fact that the exponent in the regression equation is less than 2 implies that sensitivity for the centre does not decrease in direct proportion to the centre radius. When KC cells are tested separately, the regression equation (not drawn) is:

$$K_c = 0.483 r_c^{-1.924} \ (r^2 = 0.49,\ P < 0.02),$$

As shown in Fig. 5*B*, the relationship of surround sensitivity to surround area is somewhat steeper (for all cells, $K_s = 0.11 r_s^{-2.898}$, $r^2 = 0.73$, $P < 0.02$; for KC cells, $K_s = 0.159 r_s^{-2.912}$, $r^2 = 0.76$, $P < 0.02$). We conclude that the approximately inverse relationship between contrast sensitivity and centre or surround area is common to the receptive field organisation of KC, PC and MC pathway cells.

Suppressive surround

Early studies in cat showed that the maintained and visually evoked activity of LGN cells are reduced by stimulation of regions of visual space which extend beyond the classical centre–surround receptive field (the 'suppressive field': Wiesel & Hubel, 1966; Cleland *et al.* 1971). Contrast sensitivity of marmoset LGN cells for spatially extended stimuli (Yeh *et al.* 1995; Kremers & Weiss, 1997; present results) is low in comparison to values given for macaque ganglion cells and marmoset optic tract axons (Lee *et al.* 1989; Yeh *et al.* 1995), and some PC and KC pathway cells in the current study were not at all responsive to grating stimuli presented in large (8 or 12 deg) apertures. We asked whether these effects are consistent with the action of a suppressive field. Three PC, one MC and two KC cells were tested with gratings of fixed spatial frequency presented in a range of aperture sizes. Background luminance was held constant at the average grating luminance. All cells tested showed a reduction of 20–40 % in response amplitude when the grating aperture extended beyond the dimensions of the classical receptive field centre and surround. Example responses are

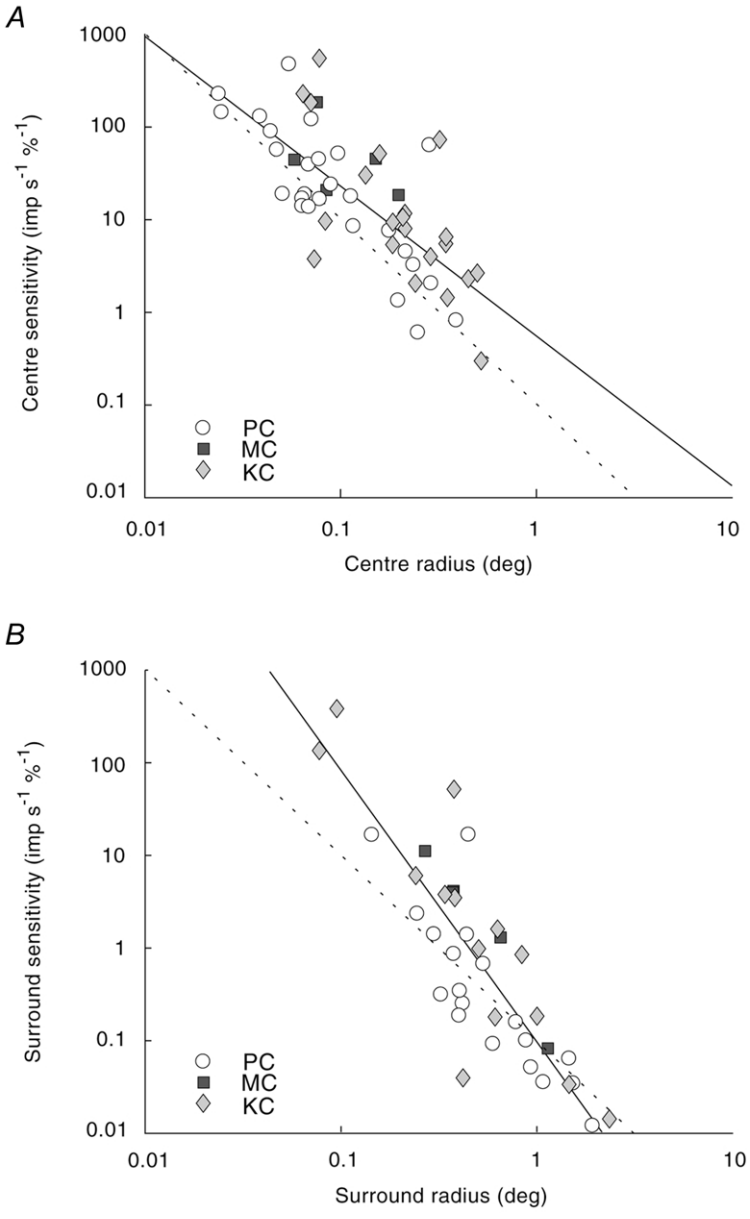

Figure 5. Centre and surround sensitivity relationships in PC, KC and MC cells

Stimulus contrast was within the linear response range for each cell. *A*, centre sensitivity (K_c) as a function of centre radius (r_c) on a double logarithmic scale. The continuous regression line has the equation $K_c = 0.62 r_c^{-1.581}$, $r^2 = 0.48$, $P < 0.02$. The dashed line shows the relationship $K_c = r_c^{-2}$. *B*, surround sensitivity as a function of surround radius. $K_s = 0.11 r_s^{-2.898}$, $r^2 = 073$, $P < 0.02$. The slope of the regression line is steeper than for the receptive field centre. The dotted line shows the relationship $K_s = r_s^{-2}$.

shown in Fig. 6 for one KC cell (Fig. 6*A* and *B*) and one PC cell (Fig. 6*C* and *D*). Each cell was also tested with an annular grating of the same spatial frequency, with inner diameter set close to the surround diameter calculated from the DOG model. Such annuli produced no response modulation (filled circle in Fig. 6*A* and *C*). These data show that a suppressive field is a feature of marmoset LGN cells. Comparison of spatial frequency tuning curves taken using small or large apertures (Fig. 6*B* and *D*) shows that the spatial transfer properties as well as the overall responsiveness of LGN cells can be affected by the suppressive field. This is consistent with our observation that some cells which responded to small, high contrast hand-held stimuli showed only feeble responses to large-field gratings. A more comprehensive analysis of this mechanism is beyond the scope of the present study.

Comparison of different koniocellular layers

Anatomical and immunohistochemical studies in several primate species (reviewed by Hendry & Reid, 2000) as well as physiological studies in *Aotus* (Xu *et al.* 2001) suggest that different KC layers may contain cells with distinct properties. A comparison of the properties of cells in the more ventral KC layers (S and Imm, nomenclature of Kaas *et al.* 1978) with those in the more dorsal KC layers (Ipm and Ipp) is shown in Fig. 7.

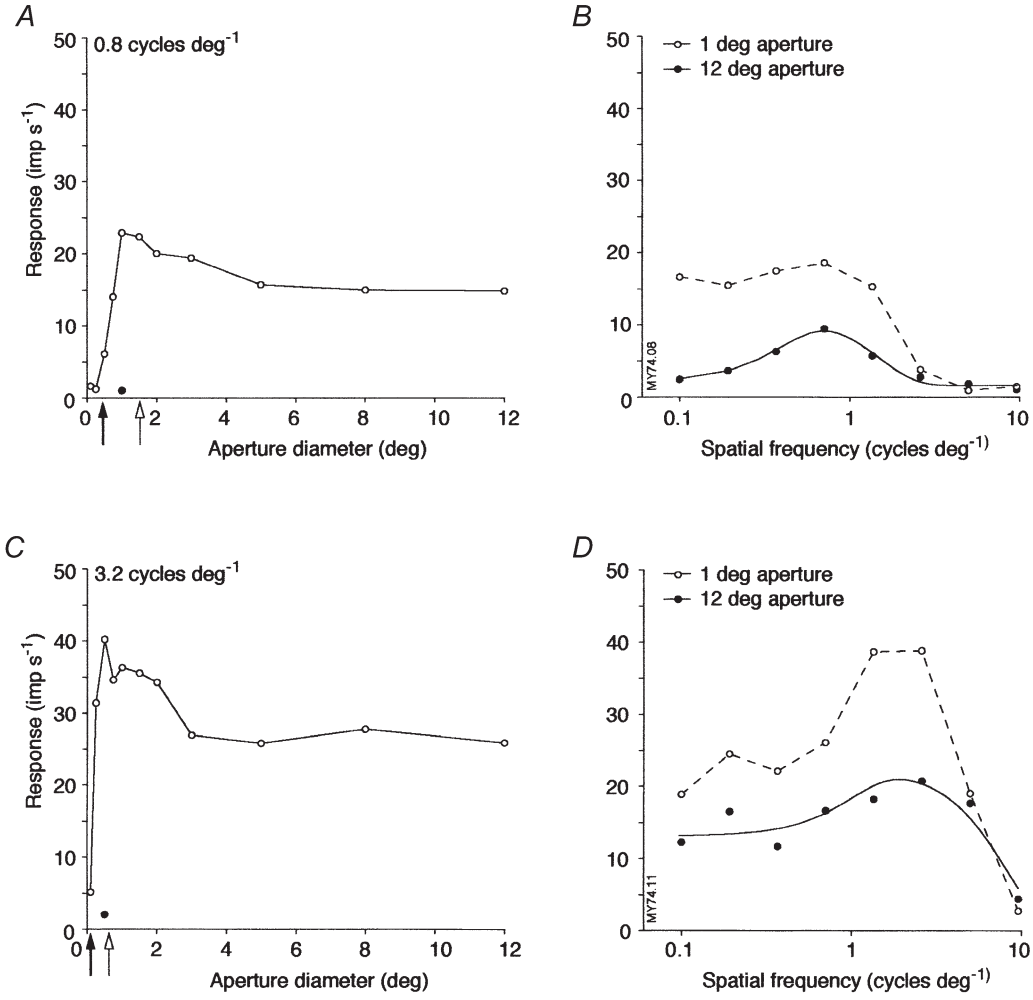

Figure 6. Evidence for the action of a suppressive field

Responses of one KC cell (*A* and *B*) and one PC cell (*C* and *D*) are shown. *A* and *C*, response amplitude for gratings presented at the optimal and temporal spatial frequency and orientation, in circular apertures. The filled and open arrows on the ordinate show the diameter of centre and surround returned by the DOG model for each cell. Response suppression is evident with increasing aperture size: the suppression from peak amplitude is 40% for the KC cell and 35% for the PC cell. The filled circles in *A* and *C* show response amplitude for an annulus at the inner diameter indicated. *B* and *D*, spatial frequency tuning curves for large (●) and small (○) apertures. Continuous lines show the DOG model fit for the large aperture. The model output has been transformed to response amplitude at the contrast level used. The tuning curves in small apertures show a generalised increase in responsivity, as well as changes in the shape of the spatial frequency tuning curve: in a small aperture the low-frequency roll-off is reduced in the KC cell (*B*) but increased in the PC cell (*D*).

Data from PC and MC cells are shown for comparison. The temporal sensitivity measurements include some data from our previous study (Solomon *et al.* 1999).

The receptive field centre radius calculated from application of the DOG model is shown in Fig. 7*A*. On average, the cells from the more ventral KC layers have the largest centre radii (0.36 deg, S.D. 0.16) and PC cells the smallest (0.12 deg, S.D. 0.02). Cut-off spatial frequency was calculated from centre radius as:

$$\text{Cut-off} = \frac{\sqrt{(\ln\pi + \ln K_c + 2\ln r_c - \text{threshold})}}{\pi r_c}, \qquad (3)$$

Where threshold was set to 0.05 imp s^{-1} $\%^{-1}$ contrast, and other symbols are as in eqn (2). The cut-off spatial frequency for PC, MC, KC (Ipp, Ipm) and KC (Imm, S) cells is shown in Fig. 7*B*. The PC and MC cells have similar, relatively high cut-off (PC: 9.24, S.D. 6.55 cycles deg^{-1}; MC: 7.76, S.D. 3.21 cycles deg^{-1}) and the ventral KC layers had the lowest (KC (Ipm, Ipp): 4.95, S.D. 3.43 cycles deg^{-1}; KC (Imm, S): 2.22, S.D. 1.22 cycles deg^{-1}). This result also confirms the differences between KC, PC and MC populations in spatial resolution as estimated from high contrast gratings (see above, Fig. 3). Such mean values must, however, be treated with caution because the proportion of cells for different eccentricities are not exactly matched (see Fig. 3), and the sample of MC cells (n =5) is small.

Our qualitative observations using hand-held stimuli suggested that KC cells in the ventral (S) layer had higher

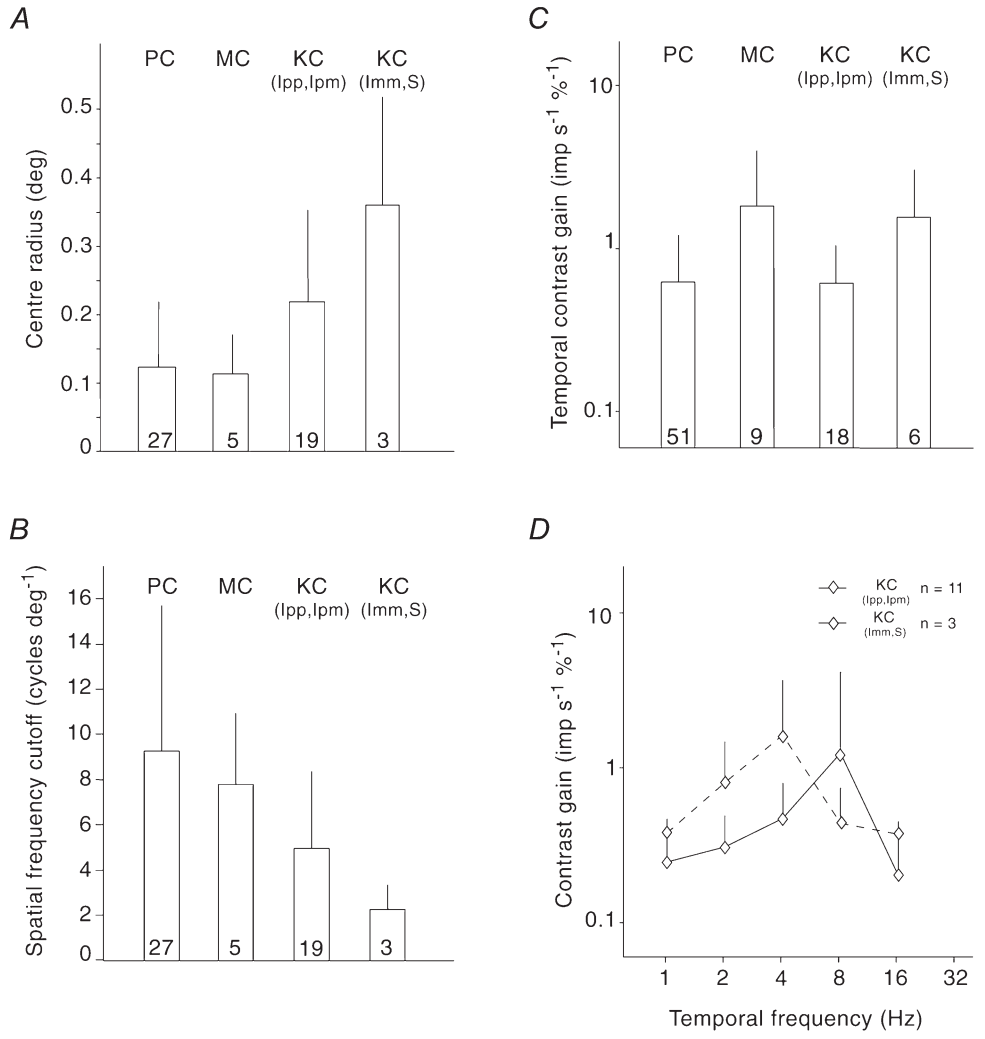

Figure 7. Summary of receptive field properties of KC cells, as compared to PC and MC cells

Error bars show 1 standard deviation. Mean receptive field centre radius (deg) calculated from the DOG model is shown in *A*. Mean receptive field centre radius (deg): PC: 0.12, S.D. 0.10; MC: 0.11, S.D. 0.06; KC (Ipp, Ipm): 0.22, S.D. 0.13; KC (Imm, S): 0.36, S.D. 0.16. Cut-off spatial frequency is shown in *B*. Mean values are: PC: 9.24, S.D. 6.55; MC: 7.76, S.D. 3.21; KC (Ipp, Ipm): 4.95, S.D. 3.43; KC (Imm, S): 2.22, S.D. 1.22. Temporal contrast gain (imp s^{-1} $\%^{-1}$) for uniform spatial modulation at 3.96 Hz. Mean values: PC: 0.63, S.D. 0.63; MC: 2.02, S.D. 2.27; KC (Ipp, Ipm) 0.63, S.D. 0.47; KC (Imm, S): 1.59, S.D. 1.50. *D*, average temporal modulation transfer functions for dorsal KC cells (Ipp, Ipm) compared with that of ventral KC (Imm, S) cells.

contrast sensitivity and responded more transiently than those in the more dorsal (Ipm and Ipp) layers. This was supported by the quantitative analysis shown in Fig. 4*C* and *D*. The ventral KC (Imm, S) cells and MC cells have similar and high contrast gain for 4 Hz temporal modulation (KC (Imm, S): 1.59, S.D. 1.50; MC: 2.02, S.D. 2.27 imp s^{-1} $\%^{-1}$). The PC cells and the more dorsally located KC cells have lower contrast gains (PC: 0.63, S.D. 0.63 imp s^{-1} $\%^{-1}$; KC (Ipp, Ipm): 0.63, S.D. 0.47 imp s^{-1} $\%^{-1}$). The dorsal KC cells (KC (Ipp, Ipm)) have a peak contrast gain at a higher temporal frequency (8 Hz) but average response falls away sharply by 16 Hz (Fig. 7*D*).

Linearity of spatial summation

A small proportion of cells in primate LGN show non-linear spatial summation (Sherman *et al.* 1976; Kaplan & Shapley, 1982; Norton & Casagrande, 1982; Derrington & Lennie, 1984; Blakemore & Vital-Durand, 1986; Irvin *et al.* 1986). We tested cells in marmoset LGN for linearity of spatial summation. For each cell, we calculated the non-linearity index according to Derrington & Lennie (1984). The first (F1) and second (F2) Fourier harmonic components of the cell's response were measured for each spatial phase of the stimulus. The maximum amplitude of F1 was averaged with the amplitude of F1 at the opposite spatial phase. The F2 amplitude was averaged over all spatial phases. The ratio of average F2 to average F1 gives the non-linearity index. Stimulus phase at maximum F1 is defined as zero, and response amplitude at zero stimulus phase is defined as positive. Amplitude is defined as negative where response phase lies between $\pi/2$ and $3\pi/2$; where F2 phase was independent of stimulus phase the F2 amplitude was arbitrarily defined as positive.

Examples of responses of KC cells to counterphase gratings are shown in Fig. 8*A*–*C*. The majority of KC cells showed substantially linear spatial summation (Fig. 8*A*), with second harmonic amplitude following the amplitude of the first harmonic. For a smaller number of cells (Fig. 8*B* and *C*) the second harmonic amplitude is independent of stimulus phase and exceeds the first harmonic amplitude over part (Fig. 8*B*) or all (Fig. 8*C*) of the stimulus phase spectrum. The KC cell illustrated in Fig. 8*B* also shows response aliasing at the stimulus monitor frame rate (67 Hz). The KC cell illustrated in Fig. 8*C* was the only example of ON–OFF-type receptive field encountered. The distribution of non-linearity index (NLI) as a function of cell position within the LGN is shown in Fig. 8*D*. The majority (6/8) of cells showing substantially non-linear summation (NLI $>$ 1) are segregated to the KC (Ipm and S) and the MC layers. The mean NLI for KC cells (0.51, S.D. 0.33) and MC cells (0.52, S.D. 0.38) is greater than that for PC cells (0.38, S.D. 0.17), but the differences between the groups are not significant ($P = 0.14$; one-way ANOVA). Overall, 8/95 (8.4%) of all cells show NLI values above unity. This proportion is higher than the average proportion (4.5%) for the entire LGN reported for macaque (Kaplan & Shapley, 1982; Derrington & Lennie, 1984; Blakemore & Vital-Durand, 1986). This may be attributed to the larger proportion of KC cells in the current sample. With the exception of the ON–OFF cell encountered (Fig. 8*C*) there was no clear relationship between spatial non-linearity and any other receptive field property examined. We conclude that the majority of spatially non-linear cells are segregated to the KC and MC subdivisions of the marmoset LGN.

Orientation and directional bias in the marmoset LGN

The majority of cells in the LGN of the macaque exhibit some bias for gratings of particular orientations or direction of movement (Lee *et al.* 1979; Smith *et al.* 1990), and some PC and MC cells in marmoset LGN have elongated receptive fields (Kremers & Weiss, 1997). We asked whether orientation or direction bias was also present in the KC population in marmoset LGN.

We quantified the response of 38 cells to 16 different orientations of gratings at the optimal spatial frequency. The sample size is limited because obliquely oriented gratings were unwieldy to produce with the visual stimulator used in early experiments (see Methods). Orientation and direction selectivity indices were calculated using the summation of vectors method of Leventhal *et al.* (1995). Each of these parameters can vary between 0 (no selectivity) and 1 (perfect selectivity). Our sample had a mean orientation index value of 0.12, S.D. 0.10, range 0.01–0.44) and a mean direction index value of 0.06, S.D. 0.05; range 0.00–0.32. For comparison, the maximum values given by Leventhal *et al.* (1995) for primary visual cortex of macaque are 0.75 for orientation and 0.50 for direction selectivity. Examples of orientation tuning curves in KC cells are shown in Fig. 9. In Fig. 9*A*, one of the most selective cells encountered is shown; a much less selective KC cell is shown in Fig. 9*B*. No significant differences in orientation or direction selectivity (one-way ANOVA, orientation bias $P = 0.43$; direction bias $P = 0.49$) exist when average values for orientation or direction selectivity for the different LGN divisions are compared (Fig. 9*C*). We conclude that a small proportion of KC cell may have a high degree of direction selectivity, but there is no reason to believe that the KC population as a whole is more selective for stimulus orientation or direction than is the MC or PC population.

Separability of KC, MC and PC populations

Our results so far show that the receptive field properties of the KC cell population show substantial overlap with those of the PC and MC populations. Irvin *et al.* (1986) showed that this is also true for the KC cell population in the prosimian *Galago*, but that KC cells nevertheless could be separated from PC and MC populations when a large number of visual response properties are considered simultaneously. We asked whether the same is true of the KC population in marmoset, by subjecting the KC, PC and MC populations to multivariate analysis (Bullier & Norton, 1979; Irvin *et al.* 1986). A multi-dimensional space is first constructed, where each dimension represents a single measurement parameter. The parameters chosen were those which, by inspection, gave the best

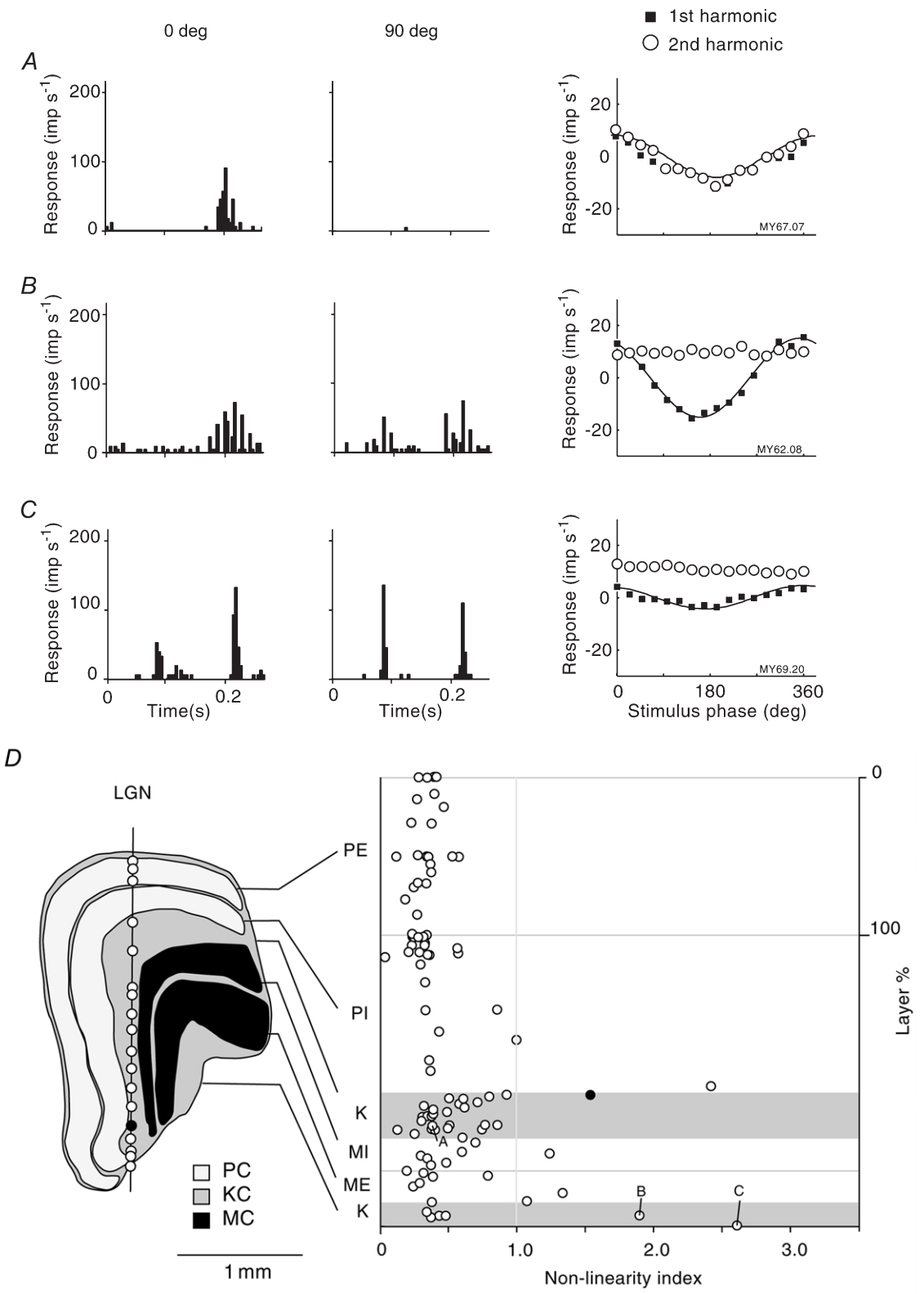

Figure 8. Spatial summation in marmoset LGN

Responses of three KC cells to counterphase gratings are shown in *A–C*. The PSTHs at two spatial phases are shown: the phase of maximum first harmonic response (left panels) and one half-cycle away from the maximum (centre panels). The right panels show first and second harmonic response amplitude as a function of spatial phase. Cell *A* shows linear spatial summation; cells *B* and *C* both show substantial 2nd response harmonic at the 1st harmonic null. The PSTH of cell *B* shows aliasing to the monitor refresh rate (67 Hz). The left panel in *D* shows a reconstructed electrode penetration through the LGN with the location of recorded cells and laminar borders. The position of one cell is highlighted (●). The right panel

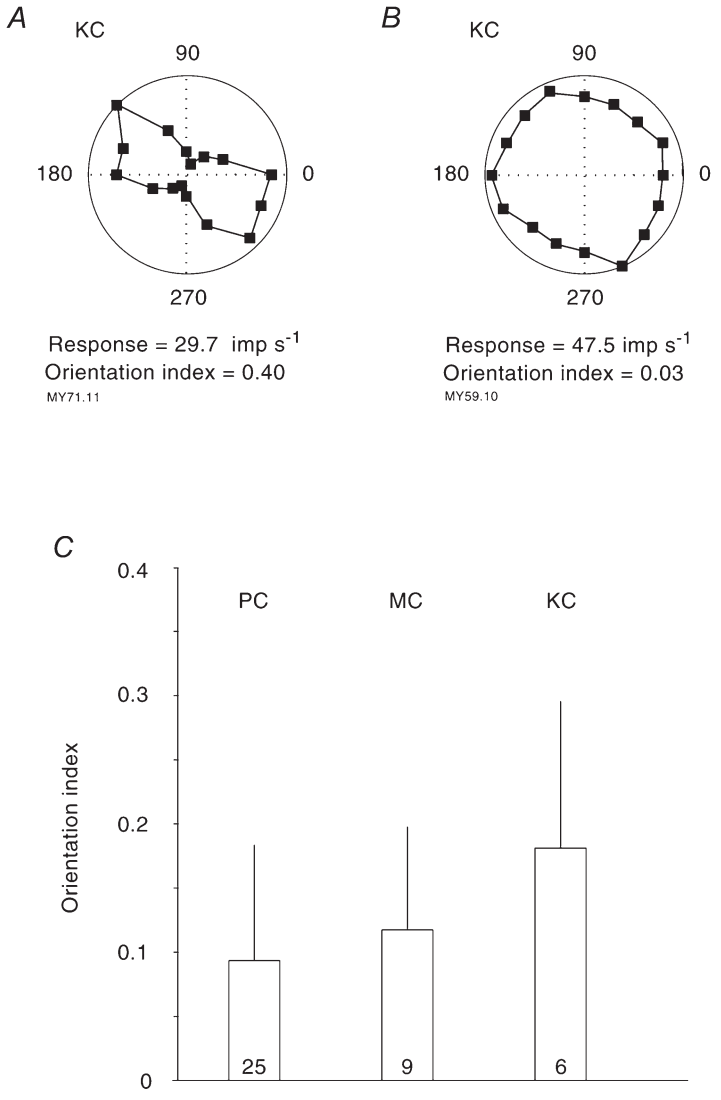

Figure 9. Orientation and direction bias in KC cells

Responses of two KC cells (*A* and *B*) to gratings presented at different orientations are shown as polar plots. Response amplitude is distance from the origin. Orientation 0 is a leftward drifting vertical grating. The cell in *A* has a large orientation bias. The cell in *B* shows no bias. Mean values for PC, KC and MC cells are shown in *C*. Error bars show standard deviation. There is no significant difference in orientation bias between the cell groups.

separation of the three cell groups. These were peak discharge rate, spontaneous discharge rate, receptive field centre integrated volume ($\pi r_c^2 k_c$), response harmonic distortion (the squared ratio of 2nd–5th harmonic to first harmonic amplitude), and spatial resolution. The harmonic distortion value was used because it gave better separation of the cell groups than the non-linearity index. The multivariate analysis rearranges this parameter space to a new space, with orthogonal dimensions (principal components) that best account for the variance in the sample population. The PC, KC and MC cell groups will occupy distinct domains within this parametric space, if the members of each group have common, yet specific, underlying determinants of their response properties. Values for each parameter were normalised to their mean, and points lying more than two standard deviations from the mean were discarded. The implications of this data selection process are considered further below. The responses of 24 KC, 30 PC and 7 MC cells met this criterion. The result is shown in Fig. 10, where the first and second principal components are plotted. The first and second components together account for 75% of the population variance (Fig. 10, inset). It is clear that there is substantial overlap between the three populations. Incorporation of other response parameters (linearity of spatial summation, direction and orientation bias, centre radius) did not substantially increase the segregation of the KC, PC and MC populations. Attempts to normalise the populations according to eccentricity-dependent regressions (see above, Results) likewise produced negligible increases in segregation of the populations. We conclude that the determinants of spatial response properties for the majority of KC, PC and MC cells show substantial commonality.

shows the non-linearity index for all tested cells plotted as a function of laminar location within the LGN. The KC layers are shaded grey. The highlighted cell (●) is located at 1% depth within the KC layer and has a non-linearity index of 1.52. The positions of the cells shown in *A*–*C* are also indicated. The majority of non-linear cells are found in the MC and ventral KC layers.

DISCUSSION

In the LGN of prosimian primates such as the bush baby, *Galago*, the KC cells form distinct layers that are segregated from the main PC and MC layers. By contrast, in simian Old World primates such as macaque or human, the KC cells comprise thin bands which are intercalated between the main MC and PC layers (Kaas *et al.* 1978; Casagrande, 1994). The extent of segregation of the KC layers in marmoset is intermediate between these two extremes (Kaas *et al.* 1978; Spatz, 1978; Goodchild & Martin, 1998; White *et al.* 1998). It is important to note in the following that although the segregation of the KC layers in marmoset is more complete than in macaque, a proportion of relay cells which are anatomically located in the PC division of the marmoset LGN could still be functionally part of the KC pathway, and *vice versa*. Furthermore, we have assessed the responses to a restricted range of spatial stimuli (i.e. spatially non-discrete achromatic gratings). Both these factors will tend to reduce the differences seen between different subdivisions of the LGN.

Receptive field dimensions

The receptive field dimensions of PC and MC cells are compatible with those reported elsewhere for marmoset (Kremers & Weiss, 1997). There is greater variability in the size of the KC receptive fields than in the size of MC and PC receptive fields (Figs 3 and 7). Analogous variability in the KC population was reported for the prosimian *Galago* (Norton & Casagrande, 1982; Conley *et al.* 1985; Irvin *et al.* 1986). In *Galago*, the receptive fields of KC cells are consistently larger than those of PC or MC cells (Norton & Casagrande, 1982; Irvin *et al.* 1986). By contrast, in marmoset we found a large degree of overlap of KC cell receptive field size with that of PC and MC cells (Figs 3, 5 and 7). This could be a general difference between simian and prosimian primates, or between nocturnal and diurnal primates. The former interpretation is supported by recent studies by Xu *et al.* (2001), who reported substantial overlap in receptive field size of KC cells with PC and MC cells in a nocturnal simian, the owl monkey, *Aotus trivurgatus*.

Contrast sensitivity

We show that for KC cells in marmoset, as previously shown for PC and MC cells in this species (Kremers & Weiss, 1997), the peak contrast sensitivity of both the centre and surround mechanisms is greater in cells with small receptive fields than in cells with large receptive fields (Fig. 5). This relationship holds to a greater or lesser extent for all concentric centre–surround visual receptive fields described so far (for cat X and Y cells: Enroth-Cugell & Shapley, 1973; Linsenmeier *et al.* 1982; Enroth-Cugell & Freeman, 1987; Macaque MC and PC cells: Croner & Kaplan, 1995; and *Galago* KC, PC and MC cells: Irvin *et al.* 1993). In marmoset, there is a less-than-proportional decrease in sensitivity of the centre mechanism with centre radius (Fig. 5*A*). This would cause cells with larger receptive fields to have greater sensitivity to diffuse illumination than cells with small receptive fields. This is consistent with our previous results from marmoset LGN, obtained from modulation of large (6.4 deg), spatially uniform fields (Solomon *et al.* 1999), and with other results from prosimian (Irvin *et al.* 1993) and simian primates (Derrington & Lennie, 1984; Croner & Kaplan, 1995). As suggested by Irvin *et al.* (1993), these fundamental aspects of ganglion cell

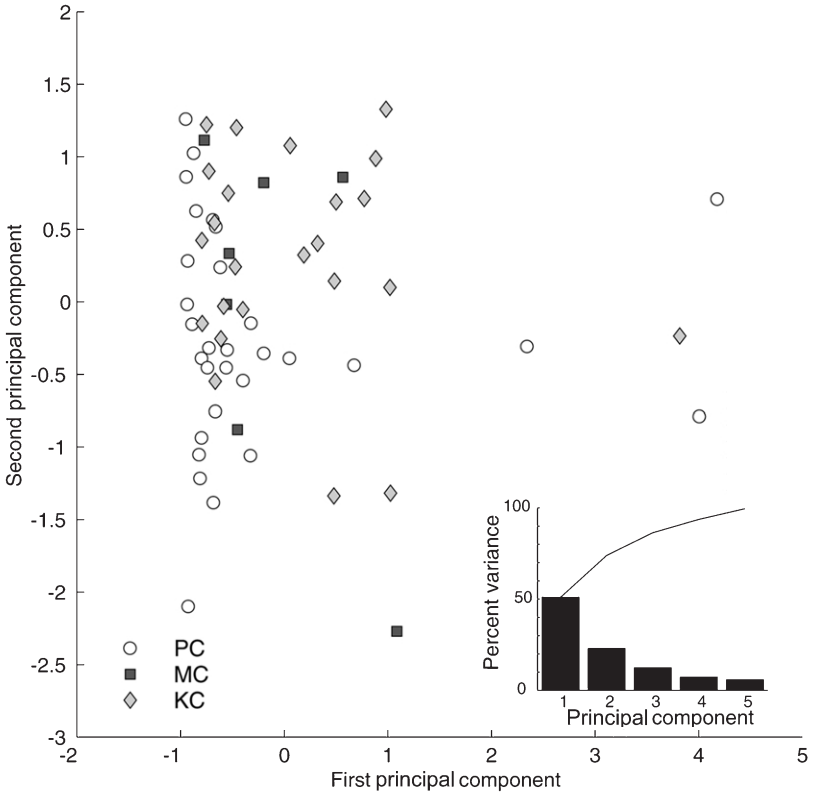

Figure 10. Non-separability of LGN cell groups

The result of multivariate (principal component) analysis is shown. The response parameters used (see text for list) were those along which the responses of KC, PC and MC cells were best segregated. The graph shows the first and second principal components. There is substantial overlap of the KC, PC and MC populations. The inset shows the proportions of total population variance accounted for by each principal component (filled bars) and as a cumulative proportion (line). The first and second principal components account for 75% of the variance in the data.

performance appear to be determined at an early level of visual processing. Current anatomical knowledge would suggest a locus in the retina at the divergence of the cone photoreceptor signal to the multiple bipolar cell types, which transmit signals to the different functional classes of ganglion cells (reviewed by Wässle, 1999).

Unresponsive cells

A proportion of cells encountered (5/84) did not respond at all to the sine wave grating stimulus. Furthermore, no evidence for the activity of a surround mechanism was given by the DOG model for 24% of cells overall. We find no clear segregation of such 'centre only' cells to the KC layers as reported for *Aotus* and *Galago* (Norton & Casagrande, 1982; Irvin *et al.* 1986; Xu *et al.* 2001). This discrepancy is probably not due to differences in classification criteria in the different studies. Cells showing no evidence of a surround in *Galago* showed poor responsivity overall (Irvin *et al.* 1986). In our sample from marmoset, the mean sensitivity (K_c) of cells where no surround could be detected (51.14, S.D. 113.56) was lower than the K_c of cells showing standard centre–surround organisation (55.26, S.D. 98.24), but this difference is not significant ($P = 0.44$, t test).

We suggest that these results can be attributed to the action of a suppressive field, which can reduce the responsivity of cells to large-field stimuli to levels close to zero (Fig. 6*A* and *C*). The inhibitory action of the 'classical' surround mechanism then has relatively little, or no effect on discharge rate and thus is less easy to detect (Fig. 6*D*, see also Levick, 1996). All cells tested in this study, as well as in ongoing work in our laboratory (S. G. Solomon, A. J. R. White & P. R. Martin, unpublished observations), show some degree of suppression for large-field stimuli. Visually unresponsive cells were reported for the KC layers in marmoset (Kremers & Weiss, 1997; Solomon *et al.* 1999), *Galago* (Norton & Casagrande, 1982; Irvin *et al.* 1986) and *Aotus* (Xu *et al.* 2001). The relationship between these descriptions, and other reports of the suppressive effects of large stimulus fields on tonic W cells (Rowe & Cox, 1993) and the 'suppressed by contrast' cell type in cat retina and LGN (Rodieck & Stone, 1965; Hoffmann *et al.* 1972; Cleland *et al.* 1976) is unclear. For the present we note that there is no clear segregation of the effect to KC cells in marmoset LGN.

Linearity of spatial summation

In all primates described so far (Kaplan & Shapley, 1982; Norton & Casagrande, 1982; Derrington & Lennie, 1984; Blakemore & Vital-Durand, 1986; Kremers & Weiss, 1997), the proportion of cells showing non-linear spatial summation is lower than that in cat, where all the (brisk-transient) Y cells and a proportion of W cells show non-linear spatial summation (Enroth-Cugell & Robson, 1966; Stone & Fukuda, 1974; Enroth-Cugell & Freeman, 1987). The possibility that non-linear cells in macaque could include KC cells was considered in previous studies (Kaplan & Shapley, 1982; Derrington & Lennie, 1984; Blakemore & Vital-Durand, 1986) but could not be resolved because the KC cells are intercalated with the other geniculate layers to a greater extent in macaque than in marmoset. The KC layers in the prosimian LGN (Norton *et al.* 1988), and the ventral C layers in the cat LGN, also contain a high proportion of cells showing Y-like spatial summation (Norton *et al.* 1988; Casagrande, 1994). However, other temporal (Solomon *et al.* 1999) and spatial properties of KC cells (present study) are more like those of PC and MC cells.

Orientation bias

Sporadic examples of cells showing direction selectivity in the KC layers of *Galago*, and the well-documented connections between the KC layers and the superior colliculus (for review, see Casagrande, 1994) encouraged us to search for direction- and orientation-selective cells in the KC layers of the marmoset. In both primate and cat, direction and orientation bias are believed to originate in the retina (Levick & Thibos, 1982; Soodak, 1987; Smith *et al.* 1990). The strength of orientation and directional bias in marmoset LGN is low compared to that described in the macaque visual cortex using the same method (Leventhal *et al.* 1995). The orientation and direction bias seen is not significantly higher in members of the KC pathway.

Conclusion

Our results substantially confirm, for a simian primate, conclusions drawn from studies of the prosimian *Galago* (Norton & Casagrande, 1982; Irvin *et al.* 1986; Norton *et al.* 1988). A substantial proportion of KC cells in marmoset have spatial properties very similar to those of PC and MC cells. The majority of KC cells respond well to conventional stimuli such as drifting gratings (this study) or Maxwellian flicker photometry (Solomon *et al.* 1999). The majority of KC cells have receptive field sizes comparable to MC and PC cells, and they share a similar relationship between receptive field size and contrast sensitivity. The feature by which KC cells are most readily distinguished from PC and MC cells is that KC cells have low peak evoked response rates and low levels of spontaneous activity (Fig. 3). This distinction is the same as the venerable distinction between sluggish and brisk populations in cat LGN (Hoffmann *et al.* 1972; Cleland *et al.* 1976).

The multivariate analysis (Fig. 10) suggests that the properties of the PC, KC and MC populations show greater overlap in the marmoset than in *Galago*. This conclusion must be given with two limitations. First, unlike Irvin *et al.* (1986) we did not include orthodromic or antidromic activation latencies in our analysis, and these parameters are good discriminators for the different cell groups. Second, in our analysis we discarded cells which deviated by more than two standard deviations from the mean value on any parameter. This step prevents any single cell from 'driving' the lower order principal components, but would eliminate any subpopulation of KC cells which is represented by only one or two members.

In terms of greater heterogeneity of receptive field size, and the presence of some cells showing significant spatial non-linearity or orientation selectivity, some members of the KC

population appear quite distinct from the PC and MC populations, and our stimulus set would not have revealed many other aspects of the cells' performance. Our sample size of KC cells is the largest recorded, to our knowledge, in any study to date. Nevertheless we cannot rule out the possibility that the small numbers of non-linear and orientation-selective cells are representatives of functionally distinct subpopulations of KC cells. We previously showed that a subpopulation of KC cells is part of the blue-On pathway for chromatic signals (White *et al.* 1998). In that study a large sample of LGN cells could be probed along a single (blue-yellow) stimulus dimension in order to activate selectively the target subpopulation. Further progress in study of the KC population might depend on the development of similar strategies using stimuli in the spatial domain.

Bishop, P. O. (1984). Processing of visual information within the retinostriate system. *Handbook of Physiology*, section 1, *The Nervous System*, vol. III, *Sensory Processes*, ed. Darian-Smith, I., pp. 341–424, American Physiological Society, Washington, DC.

Bishop, P. O., Burke, W. & Davis, R. (1962). The interpretation of the extracellular response of lateral geniculate cells. *Journal of Physiology* **162**, 451–472.

Blakemore, C. & Vital-Durand, F. (1986). Organization and post-natal development of the monkey's lateral geniculate nucleus. *Journal of Physiology* **380**, 453–491.

Brainard, D. H. (1997). The Psychophysics Toolbox. *Spatial Vision* **10**, 443–446.

Bullier, J. & Norton, T. T. (1979). Comparison of receptive-field properties of X and Y lateral geniculate cells in the cat. *Journal of Neurophysiology* **42**, 274–291.

Casagrande, V. A. (1994). A third parallel visual pathway to primate area V1. *Trends in Neurosciences* **17**, 305–310.

Casagrande, V. A. & Norton, T. T. (1991). Lateral geniculate nucleus: a review of its physiology and function. In *Vision and Visual Dysfunction*, vol. 4, *The Neural Basis of Visual Function*, ed. Leventhal, A. G., pp. 41–84. Macmillan Press, New York.

Cleland, B. G. (1983). Sensitivity to stationary flashing spots of the brisk classes of ganglion cells in the cat retina. *Journal of Physiology* **345**, 15–26.

Cleland, B. G., Dubin, M. W. & Levick, W. R. (1971). Sustained and transient neurones in the cat's retina and lateral geniculate nucleus. *Journal of Physiology* **217**, 473–496.

Cleland, B. G., Levick, W. R., Morstyn, R. & Wagner, H. G. (1976). Lateral geniculate relay of slowly-conducting retinal afferents to cat visual cortex. *Journal of Physiology* **255**, 299–320.

Conley, M., Birecree, E. & Casagrande, V. A. (1985). Neuronal classes and their relation to functional and laminar organization of the lateral geniculate nucleus: a Golgi study of the prosimian primate, *Galago crassicaudatus*. *Journal of Comparative Neurology* **242**, 561–583.

Croner, L. J. & Kaplan, E. (1995). Receptive fields of P and M ganglion cells across the primate retina. *Vision Research* **35**, 7–24.

Derrington, A. M. & Lennie, P. (1984). Spatial and temporal contrast sensitivities of neurones in lateral geniculate nucleus of macaque. *Journal of Physiology* **357**, 219–240.

Ding, Y. & Casagrande, V. A. (1997). The distribution and morphology of LGN K pathway axons within the layers and CO blobs of owl monkey V1. *Visual Neuroscience* **14**, 691–704.

Enroth-Cugell, C. & Freeman, A. W. (1987). The receptive-field spatial structure of cat retinal Y cells. *Journal of Physiology* **384**, 49–79.

Enroth-Cugell, C. & Robson, J. (1966). The contrast sensitivity of retinal ganglion cells of the cat. *Journal of Physiology* **187**, 517–552.

Enroth-Cugell, C. & Shapley, R. M. (1973). Flux, not retinal illumination, is what cat retinal ganglion cells really care about. *Journal of Physiology* **233**, 311–326.

Goodchild, A. K., Ghosh, K. K. & Martin, P. R. (1996). Comparison of photoreceptor spatial density and ganglion cell morphology in the retina of human, macaque monkey, cat, and the marmoset *Callithrix jacchus*. *Journal of Comparative Neurology* **366**, 55–75.

Goodchild, A. K. & Martin, P. R. (1998). The distribution of calcium binding proteins in the lateral geniculate nucleus and visual cortex of a New World monkey, the marmoset *Callithrix jacchus*. *Visual Neuroscience* **15**, 625–642.

Hendry, S. C. & Reid, R. C. (2000). The koniocellular pathway in primate vision. *Annual Review of Neuroscience* **23**, 127–153.

Hoffmann, K. P., Stone, J. & Sherman, S. M. (1972). Relay of receptive-field properties in dorsal lateral geniculate nucleus of the cat. *Journal of Neurophysiology* **35**, 518–531.

Irvin, G. E., Casagrande, V. A. & Norton, T. T. (1993). Center/surround relationships of magnocellular, parvocellular, and koniocellular relay cells in primate lateral geniculate nucleus. *Visual Neuroscience* **10**, 363–373.

Irvin, G. E., Norton, T. T., Sesma, M. A. & Casagrande, V. A. (1986). W-like response properties of interlaminar zone cells in the lateral geniculate nucleus of a primate (*Galago crassicaudatus*). *Brain Research* **362**, 254–270.

Kaas, J. H., Huerta, M. F., Weber, J. T. & Harting, J. K. (1978). Patterns of retinal termination and laminar organization of the lateral geniculate nucleus in primates. *Journal of Comparative Neurology* **182**, 517–554.

Kaplan, E., Lee, B. B. & Shapley, R. M. (1989). New views of primate retinal function. In *Progress in Retinal Research*, ed. Osborne, N. & Chader, J., pp. 273–336. Pergamon, New York.

Kaplan, E. & Shapley, R. M. (1982). X and Y cells in the lateral geniculate nucleus of macaque monkeys. *Journal of Physiology* **330**, 125–143.

Kremers, J. & Weiss, S. (1997). Receptive field dimensions of lateral geniculate cells in the common marmoset (*Callithrix jacchus*). *Vision Research* **37**, 2171–2181.

Kremers, J., Weiss, S. & Zrenner, E. (1997). Temporal properties of marmoset lateral geniculate cells. *Vision Research* **37**, 2649–2660.

Le Gros Clark, W. E. (1941). The lateral geniculate body in the platyrrhine monkeys. *Journal of Anatomy* **76**, 131–140.

Lee, B. B. (1996). Receptive field structure in the primate retina. *Vision Research* **36**, 631–644.

Lee, B. B., Creutzfeldt, O. D. & Elepfandt, A. (1979). The responses of magno- and parvocellular cells of the monkey's lateral geniculate body to moving stimuli. *Journal of Neurophysiology* **35**, 547–557.

Lee, B. B., Martin, P. R. & Valberg, A. (1989). Sensitivity of macaque retinal ganglion cells to chromatic and luminance flicker. *Journal of Physiology* **414**, 223–243.

Leventhal, A. G., Thompson, K. G., Liu, D., Zhou, Y. & Ault, S. J. (1995). Concomitant sensitivity to orientation, direction, and color of cells in layers 2, 3, and 4 of monkey striate cortex. *Journal of Neuroscience* **15**, 1808–1818.

Levick, W. R. (1996). Receptive fields of cat retinal ganglion cells with special reference to the alpha cells. *Progress in Retinal and Eye Research* **15,** 457–500.

Levick, W. R. & Thibos, L. N. (1982). Analysis of orientation bias in cat retina. *Journal of Physiology* **329**, 243–261.

Linsenmeier, R. A., Frishman, L. J., Jakiela, H. G. & Enroth-Cugell, C. (1982). Receptive field properties of X and Y cells in the cat retina derived from contrast sensitivity measurements. *Vision Research* **22**, 1173–1183.

Martin, P. R., White, A. J. R. & Solomon, S. G. (1999). Spatial properties of koniocellular cells in the primate lateral geniculate nucleus. *Investigative Ophthalmology and Visual Science* (*ARVO abstracts*) **40**, 993.

Naka, K.-I. & Rushton, W. H. (1966). S-potentials from colour units in the retina of fish (*Cyprinida*). *Journal of Physiology* **185**, 536–555.

Norton, T. T. & Casagrande, V. A. (1982). Laminar organization of receptive-field properties in lateral geniculate nucleus of bush baby (*Galago crassicaudatus*). *Journal of Neurophysiology* **47**, 715–741.

Norton, T. T., Casagrande, V. A., Irvin, G. E., Sesma, M. A. & Petry, H. M. (1988). Contrast-sensitivity functions of W-, X-, and Y-like relay cells in the lateral geniculate nucleus of bush baby, *Galago crassicaudatus*. *Journal of Neurophysiology* **59**, 1639–1656.

Ordy, J. M. & Samorajski, T. (1968). Visual acuity and ERG-CFF in relation to the morphologic organization of the retina among diurnal and nocturnal primates. *Vision Research* **8**, 1205–1225.

Rodieck, R. W. (1965). Quantitative analysis of cat retinal ganglion cell response to visual stimuli. *Vision Research* **5**, 583–601.

Rodieck, R. W. & Stone, J. (1965). Response of cat retinal ganglion cells to moving visual patterns. *Journal of Neurophysiology* **28**, 819–832.

Rowe, M. H. & Cox, J. F. (1993). Spatial receptive-field structure of cat retinal W cells. *Visual Neuroscience* **10**, 765–779.

Sherman, S. M., Wilson, J. R., Kaas, J. H. & Webb, S. V. (1976). X- and Y-cells in the dorsal lateral geniculate nucleus of the owl monkey (*Aotus trivirgatus*). *Science* **192**, 475–477.

Smith, E. L. I., Chino, Y. M., Ridder, W. H. I., Kitagawa, K. & Langston, A. (1990). Orientation bias of neurons in the lateral geniculate nucleus of macaque monkeys. *Visual Neuroscience* **5**, 525–545.

Solomon, S. G., White, A. J. R. & Martin, P. R. (1999). Temporal sensitivity in the lateral geniculate nucleus of a New World monkey, the marmoset *Callithrix jacchus*. *Journal of Physiology* **517**, 907–917.

Soodak, R. E. (1987). The retinal ganglion cell mosaic defines orientation columns in striate cortex. *Proceedings of the National Academy of Sciences of the USA* **84**, 3936–3940.

Spatz, W. B. (1978). The retino-geniculo-cortical pathway in *Callithrix*. I. Intraspecific variations in the lamination pattern of the lateral geniculate nucleus. *Experimental Brain Research* **33**, 551–563.

Stephan, H., Baron, G. & Schwerdtfeger, W. K. (1980). *The Brain of the Common Marmoset* (*Callithrix jacchus*). *A Stereotaxic Atlas.* Springer, Berlin.

Stone, J. & Fukuda, Y. (1974). Properties of cat retinal ganglion cells: a comparison of W-cells with X- and Y-cells. *Journal of Neurophysiology* **37**, 722–748.

Troilo, D., Howland, H. C. & Judge, S. J. (1993). Visual optics and retinal cone topography in the common marmoset (*Callithrix jacchus*). *Vision Research* **33**, 1301–1310.

Usrey, W. M. & Reid, R. C. (2000). Visual physiology of the lateral geniculate nucleus in two species of New World monkey: *Saimiri sciureus* and *Aotus trivirgatis*. *Journal of Physiology* **523**, 755–769.

Walls, G. L. (1953). *The Lateral Geniculate Nucleus and Visual Histophysiology.* University of California Press, Berkeley, CA, USA.

Wässle, H. (1999). Mammalian rod and cone pathways. *The Retinal Basis of Vision*, ed. Toyoda, J., Motohiko, M., Kaneko, A., Saito, T. & Murakami, M., pp.185–195. Elsevier Science B.V., Amsterdam.

White, A. J. R., Goodchild, A. K., Wilder, H. D., Sefton, A. E. & Martin, P. R. (1998). Segregation of receptive field properties in the lateral geniculate nucleus of a New-World monkey, the marmoset *Callithrix jacchus*. *Journal of Neurophysiology* **80**, 2063–2076.

Wiesel, T. N. & Hubel, D. H. (1966). Spatial and chromatic interactions in the lateral geniculate body of the rhesus monkey. *Journal of Neurophysiology* **29**, 1115–1156.

Wilder, H. D., Grunert, U., Lee, B. B. & Martin, P. R. (1996). Topography of ganglion cells and photoreceptors in the retina of a New World monkey: the marmoset *Callithrix jacchus*. *Visual Neuroscience* **13**, 335–352.

Xu, X., Ichada, J., Allison, J. D., Bonds, A. B. & Casagrande, V. A. (2001). A comparison of the koniocellular (K), magnocellular (M) and parvocellular (P) receptive field properties in the lateral geniculate nucleus (LGN) of the owl monkey (*Aotus trivirgatus*). *Journal of Physiology* **531**, 203–218.

Yeh, T., Lee, B. B., Kremers, J., Cowing, J. A., Hunt, D. M., Martin, P. R. & Troy, J. (1995). Visual responses in the lateral geniculate nucleus of dichromatic and trichromatic marmosets (*Callithrix jacchus*). *Journal of Neuroscience* **15**, 7892–7904.

Acknowledgements

We thank A. Lara for technical assistance, J. Potas for help with some experiments, and T. Tan, J. Leung and M. Razavian for software development. We thank Abbot Australasia for the kind donation of the isoflurane used in these experiments. We are grateful to Vivien Casagrande for many helpful comments on the manuscript. This work was supported by Australian NH&MRC grants 960970 and 107247 and the Lions Club Health Care Foundation. A.W. was supported by a NH&MRC Scholarship 997540. S.S. was supported by a University of Sydney, Faculty of Medicine Postgraduate Scholarship.

Corresponding author

P. R. Martin: Department of Physiology, F13, University of Sydney, NSW 2006, Australia.

Email: paulm@physiol.usyd.edu.au